Am J Physiol Gastrointest Liver Physiol 300: G598–G607, 2011.
First published January 13, 2011; doi:10.1152/ajpgi.00323.2010.

Lack of transketolase-like (TKTL) 1 aggravates murine experimental colitis

Susanne Bentz,[1] Theresa Pesch,[1] Lutz Wolfram,[1] Cheryl de Vallière,[1] Katharina Leucht,[1] Michael Fried,[1] Johannes F. Coy,[2] Martin Hausmann,[1] and Gerhard Rogler[1]

[1]*Division of Gastroenterology and Hepatology, Department of Internal Medicine, University Hospital Zurich, Zurich, Switzerland; and* [2]*Tavargenix GmbH, Darmstadt, Germany*

Submitted 8 July 2010; accepted in final form 4 January 2011

Bentz S, Pesch T, Wolfram L, de Vallière C, Leucht K, Fried M, Coy JF, Hausmann M, Rogler G. Lack of transketolase-like (TKTL) 1 aggravates murine experimental colitis. *Am J Physiol Gastrointest Liver Physiol* 300: G598–G607, 2011. First published January 13, 2011; doi:10.1152/ajpgi.00323.2010.—Transketolase-like (TKTL) 1 indirectly replenishes NADPH preventing damage induced by reactive oxygen species (ROS) formed upon intestinal inflammation. We investigated the function of TKTL1 during murine colitis and ROS detoxification for prevention of tissue damage. Mucosal damage in TKTL1$^{-/-}$ and wild-type (WT) mice was assessed by miniendoscopy and histology during dextran sodium sulfate (DSS) colitis. mRNA levels of interferon (IFN)-γ, inducible nitric oxide synthase (iNOS), interleukin (IL)-6, tumor necrosis factor (TNF), transketolase (TKT), and TKTL2 were determined by PCR and/or Western blotting. To assess oxidative and nitrosative stress nitrosylation, carbonylation and antioxidative enzymes catalase (Cat), superoxide dismutase 1 and 2, as well as glutathione (GSH) were determined. Myeloperoxidase (MPO) was determined for assessment of tissue neutrophils. TKTL1 knockout or DSS treatment did not influence TKT and TKTL2 mRNA or protein expression. Mucosal damage was significantly increased in TKTL1$^{-/-}$ mice indicated by miniendoscopy as well as a significantly shorter colon and more severe histological scores compared with WT mice during DSS colitis. This was associated with higher mRNA levels of IFN-γ, iNOS, IL-6, and TNF. In addition, iNOS protein expression was significantly enhanced in TKTL1$^{-/-}$ mice as well as MPO activity. Protein modification by nitric oxide (nitrotyrosine) was induced in TKTL1$^{-/-}$ mice. However, introduction of carbonyl groups by ROS was not induced in these mice. The expression of SOD1, SOD2, Cat, as well as GSH content was not significantly changed in TKTL1$^{-/-}$ mice. We conclude that induced colitis in TKTL1$^{-/-}$ mice was more severe compared with WT. This indicates a role of TKTL1 during mucosal repair and restoration.

redox status; aerobic glycolysis; reactive oxygen species; experimental dextran sodium sulfate colitis

REACTIVE OXYGEN SPECIES (ROS) are possible etiological factors in the initiation or development of the inflammatory process during inflammatory bowel disease (IBD), where they contribute to the damage of the intestinal mucosa (12). Low levels of endogenous antioxidants have been described in the colonic mucosa of IBD patients (17), and oxidative stress may therefore exceed the capacity of endogenous defense mechanisms, such as neutralization of ROS by the reducing agent nicotinamide adenine dinucleotide phosphate (NADPH) (13, 29). In addition to a defective ROS defense, elevated levels of proinflammatory cytokines such as tumor necrosis factor (TNF)-α (21, 24, 32), interferon (IFN)-γ (21), and interleukin (IL)-6 (24, 32) have been observed in intestinal biopsies derived from IBD patients. Furthermore, increased expression of the inducible nitric oxide synthase (iNOS) has been reported in IBD patients (2, 7) and in animal models of intestinal inflammation (22, 33).

Transketolase (TKTs) enzymes catalyze the transfer of a 2-carbon fragment, e.g., from D-xylulose 5-phosphate (*P*) to D-ribose 5-*P*, subsequently leading to the formation of sedoheptulose 7-*P* via the pentose phosphate pathway (PPP). TKTs indirectly serve to replenish the pool of endogenous antioxidants, thus preventing damage induced by ROS and free radicals formed upon inflammation (19). In contrast to lower vertebrates, higher vertebrates harbor one TKT gene as well as the transketolase-like (TKTL) 1 and TKTL2 genes (4). Whereas the function of TKT has been studied extensively (14, 27, 30, 36–38, 45–46), less is known about that of TKTL1 and TKTL2. Total TKT activity has been investigated in several organisms and tissues, for instance, in corneal cells (19, 34), colonic epithelial cells (44), endothelial cells (20, 37–38, 44–46), or *Saccharomyces cerevisiae* (26, 39). In general, TKTs require diphosphorylated thiamine (vitamin B_1) as a cofactor. Thiamine deficiency and consequent impairment in TKT activity has been suggested to play a role in several human pathological conditions, including Alzheimer's disease (36), Wernicke-Korsakoff's syndrome (30), alcoholism (14), and diabetes mellitus (36). During hyperglycemia in diabetes mellitus, ROS formation (27) is enhanced and TKT gene expression is consequently induced through the antioxidant response element (ARE)-mediated promoter activation (27, 46). Supplementation of dietary thiamine in diabetes mellitus patients could thus lead to increased TKT activity and thereby more effective neutralization of ROS by NADPH. Thiamine diphosphate prodrugs, such as benfotiamine, have been shown to prevent early renal and retinal damage in animal studies (37) and reduce neuropathic pain through a direct antioxidant effect in diabetes mellitus in clinical studies (37). Furthermore, benfotiamine exhibited direct antioxidative capacity and prevented induction of DNA damage (37). The depletion of thiamine with oxythiamine in hepatocytes of rats leads to decreased TKT activity (38).

Disruption of one TKT allele is sufficient for causing growth retardation in mice, whereas inactivation of both TKT alleles is lethal (45). In contrast, TKTL1-deficient mice are viable and have no obvious phenotype, indicating that TKTL1 executes different physiological functions. The functional difference between TKT and TKTL1 is further supported by a TKTL1-specific deletion of an exon (homologous to TKT exon 3) encoding two invariant amino acid residues present in all known TKT proteins (5). The genomic structure of the three TKT genes and the presence of the exon 3 deletion of TKTL1 in humans, mouse, and rat indicate that, during evolution of the

Address for reprint requests and other correspondence: G. Rogler, Division of Gastroenterology and Hepatology, Dept. of Internal Medicine, Univ. Hospital Zurich, Raemistrasse 100, 8091 Zurich, Switzerland (e-mail: gerhard.rogler@usz.ch).

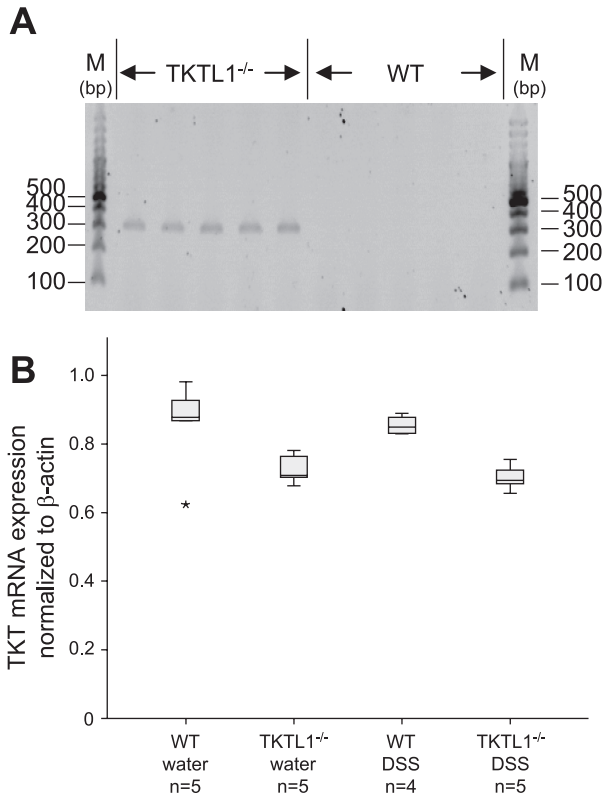

Fig. 1. *A*: genotyping PCR and electrophoretic separation of DNA isolated from colon tissue of transketolase-like (TKTL) 1 knockout (TKTL1$^{-/-}$) mice and wild-type (WT) mice. The deletion of exon 4–7 leads to a characteristic 338-bp fragment. TKTL1$^{-/-}$ mice (*left*) showed this fragment while WT mice (*right*) did not. *B*: semiquantitative PCR of transketolase (TKT) and actin as housekeeping control in colon specimens of TKTL1$^{-/-}$ mice and WT mice with and without administration of dextran sodium sulfate (DSS). TKT expression normalized to actin expression by densitometry. TKT expression is not influenced by DSS or water treatment nor the deletion of TKTL1. *Outlier (Kruskal Wallis test). M, mol wt.

vertebrate genome, this deletion occurred within the TKTL1 gene before the human and murine lineages diverged. The high similarity between TKTL1 and TKTL2 suggests that, before the deletion of exon 3, an intact copy of TKTL1 was duplicated and integrated into the genome by a reverse transcriptase-mediated event, giving rise to TKTL2 (4). In contrast to TKT and TKTL2 TKT genes, the TKTL1 gene is upregulated in tumor cells (18). TKTL1 mRNA and protein expression have been linked to metastasis and poor survival of cancer patients (6, 42). TKTL1 gene is activated by promoter hypomethylation and contributes to carcinogenesis through increased aerobic glycolysis and hypoxia-inducible factor-1α stabilization (42).

No previous studies have been reported addressing the role of TKTL1 in mice. The aim of this study was to investigate the role of TKTL1 during inflammatory processes and its potential role in ROS detoxification during experimental dextran sodium sulfate (DSS)-induced colitis.

MATERIALS AND METHODS

TKTL1 knockout mice. A TKTL1 targeting vector was electroporated into C57-BL/6 embryonic stem (ES) cells by TaconicArtemis (Cologne, Germany). Homologous recombinant ES cells were identified by Southern blotting analysis and microinjected in C57-BL/6 blastocysts. Offsprings were backcrossed to C57-BL/6 mice, and germline transmission was confirmed by PCR of tail genomic DNA. Screening of TKTL1$^{-/-}$ and TKTL1$^{+/+}$ mice by PCR genotyping was carried out using genomic DNAs isolated from mouse tails and colon tissues as templates, and the following oligonucleotides: 5′-ATGGCTCATGTTTCTGCTGC-3′ (intron 3) and 5′-CTTGCCTTGCTTCTGTAAGG-3′ (intron 7).

Induction of acute colitis. Animal experiments were carried out according to Swiss animal welfare laws and were approved by the veterinary authorities of Zurich, Switzerland. Seven- to eight-wk-old female C57BL/6J-Fue mice (wild type, WT) or female TKTL1 knockout mice (TKTL1$^{-/-}$; Taconic Europe) were used for the experiments and housed in a specified pathogen-free facility in individually ventilated cages. Acute colitis was induced with 2.5% of DSS (MP Biomedicals, Illkirch, France) in drinking water (28). The animals were randomly divided into four groups, two DSS groups and two water control groups with five individuals each. Animals were fed food and water with or without DSS ad libitum.

Determination of colonoscopy score. Animals were anesthetized intraperitoneally with a mixture of 90–120 mg/kg body wt ketamine (Vétoquinol, Bern, Switzerland) and 8 mg/kg body wt xylazine (Bayer, Lyssach, Switzerland). Animals were examined as described previously (1, 11). The solid endoscope was introduced per anus with a lubricant (2% lidocaine) in the sedated mouse. The colon was gently inflated with air. Recording was performed with the Karl Storz Tele Pack Pal 20043020 (Karl Storz Endoskope, Tuttlingen, Germany). Mucosal damage was assessed by miniendoscopy and the endoscopic colitis score murine endoscopic index of colitis severity (MEICS). We determined mucosal bleeding, altered vascular pattern, nontransparent mucosa, abundant fibrin, and unshaped or spread stool.

Determination of histological score and colon length. From the distal third of the colon, 1 cm of colonic tissue was removed and fixed

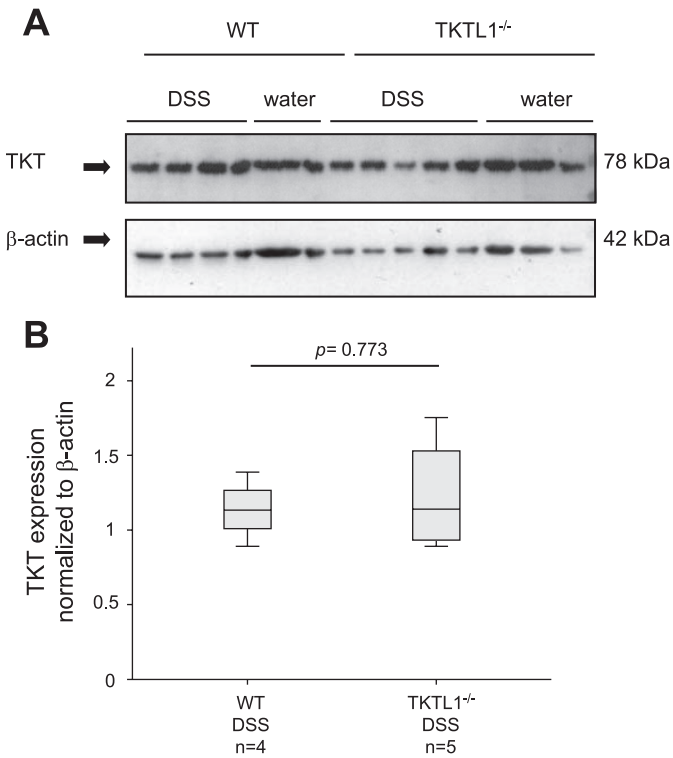

Fig. 2. *A*: Western blotting of TKT in TKTL1$^{-/-}$ mice and WT mice with and without administration of DSS. *B*: TKT expression normalized to β-actin expression by densitometry. TKT expression is not influenced by DSS or water treatment nor the deletion of TKTL1. TKTL1$^{-/-}$ mice expressed equally TKT protein compared with WT mice treated with DSS ($P = 0.773$, Mann-Whitney test).

in 4% formalin overnight. Sections of the paraffin-embedded tissue were used for histological analysis, as described previously based on the loss of goblet cells, loss of crypts, immigration of lymphocytes, thickening of submucosa/mucosa, and the number of lymph nodes (28, 41). Three sections, each obtained at 100 μm distance, were evaluated. Histological examination was performed by an independent, blinded investigator.

Genomic DNA extraction and genotyping. For genotyping, PCR analysis was performed by extracting the DNA from paraffin-embedded colon tissue. For elimination of paraffin, 10-μm sections were dissolved in xylol for 15 min at room temperature. After centrifugation at 1,500 *g* for 10 min, the cell pellet was washed two times with 70% ethanol. DNA was purified according to the manufacturer's instruction with the QIAamp DNA Mini Kit (Qiagen, Hombrechtikon, Switzerland). Genotyping was performed with the previously mentioned primers (under *TKTL1 knockout mice*). The isolated DNA (100 ng) was mixed with the Hot Start TaqPolymerase Master Mix (Qiagen), and PCR was carried out under the following cycling conditions: 15 min at 95°C, 30 s at 94°C, 30 s at 60°C, 1 min at 72°C (35 cycles), and 10 min at 70°C and separated by 2% agarose gel electrophoresis (all from Invitrogen, Basel, Switzerland). TKTL1$^{-/-}$ demonstrate a 338-bp fragment.

Semiquantitative PCR of TKT and TKTL2. To determine TKT and TKTL2 expression, cDNAs were mixed with the Hot Start TaqPolymerase Master Mix (Qiagen), and PCR was performed under the following cycling conditions: 15 min at 95°C, then 40 cycles of 94°C

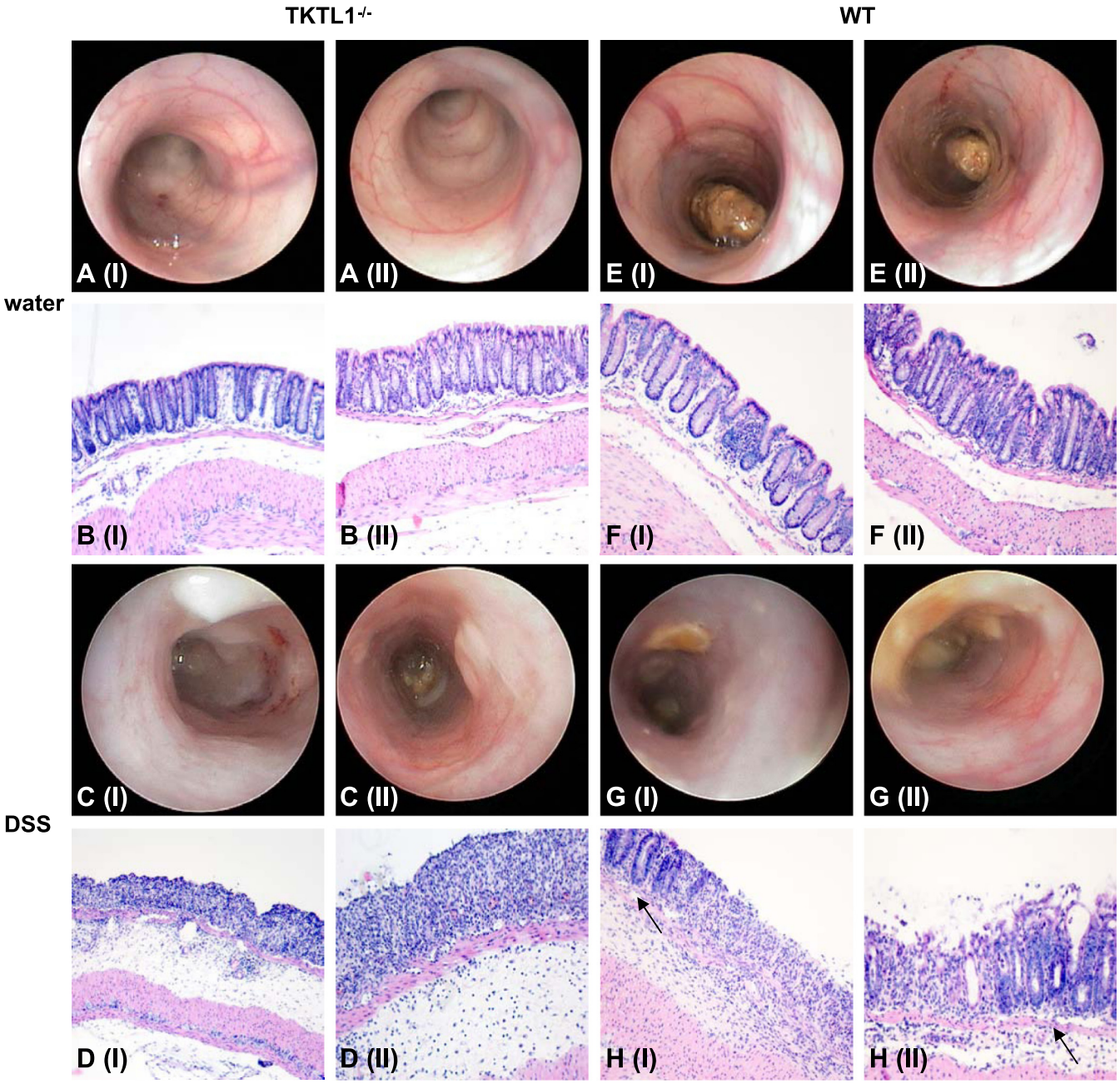

Fig. 3. Miniendoscopy of distal colon and hematoxylin and eosin staining of terminal colon. *A* and *B*, *I* and *II*: TKTL1$^{-/-}$ mice with water. *C* and *D*, *I* and *II*: TKTL1$^{-/-}$ mice treated with DSS. *E* and *F*, *I* and *II*: WT mice treated with water. *G* and *H*, *I* and *II*: WT mice treated with DSS. Less disruption of the epithelium was observed (indicated with arrows) in WT mice with DSS than in TKTL1$^{-/-}$ mice with DSS (*D* and *H*).

for 30 s, 60°C for 30 s, and 72°C for 2 min and a final extension of 70°C for 10 min. Oligonucleotide sequences were established using primer finder at the National Center for Biotechnology Information webpage: TKT 5′-CCCCCTCAGGAGGATGCCCC-3′ and 5′-CAGGACCACCTTGGCTTGGCC-3′, TKTL2 5′-CTTCGTACGGCAGCCGAGCTGC-3′ and 5′-AACGCTTGGCAGCGCTTCTCAT-3′. For a housekeeper, actin expression was determined using the following oligonucleotides: 5′-GCTCACCATGGATGATGATATCGC-3′ and 5′-GGAGGAGCAATGATCTTGATCTTC-3′ (Gene Checker; Invitrogen). Fragment separation was performed by 1% agarose gel electrophoresis (all from Invitrogen). The level of mRNA expression was evaluated by measurement of band intensity by densitometry using OptiQuant Acquisition Analysis Software (Microsoft XP) and relative quantification to actin.

RNA extraction and quantitative real-time PCR. Total RNA was isolated using the RNeasy Mini Kit and the automated sample preparation system Qiacube (Qiagen) following the manufacturer's recommendations. cDNA was synthesized with a High-Capacity cDNA Reverse Transcription Kit according to the manufacturer's instructions. To determine the iNOS, IFN-γ, IL-6, and TNF expression, quantitative real-time PCR (qRT-PCR) was performed under the following cycling conditions: 20 s at 95°C, then 45 cycles of 95°C for 3 s and 60°C for 30 s with the TaqMan Fast Universal Mastermix. Each sample was analyzed in triplicate. For a housekeeper, GAPDH expression was determined (all from Applied Biosystems, Foster City, CA). The comparative $\Delta\Delta C_t$ method was applied to determine the quantity of the target sequences relative to the endogenous control GAPDH and a reference sample.

Protein extraction and Western blotting. Whole colon tissue was homogenized in M-PER lysis buffer (Thermo Fisher Scientific) by a tissuelyzer (Qiagen, Hilden, Germany). Tissue homogenates were sonicated and centrifuged for 5 min at 13,000 *g*. Protein concentration of the soluble supernatants was determined by the Nanodrop ND UV-Vis Spectrophotometer (NanoDrop Technologies) and used for Western blotting.

Total proteins (20 μg) were separated on 4–12% Bis-Tris gradient gels with MOPS SDS running buffer (Invitrogen, Carlsbad, CA) and transferred to a nitrocellulose membrane (Invitrogen). The membranes were blocked with 5% milk powder (Roth, Karlsruhe, Germany) and 3% BSA (Sigma-Aldrich, St. Louis, MO) in a solution with 0.1% Tween 20 (Roth) in 1× PBS. Protein labeling was carried out with specific primary antibodies for iNOS, SOD1, nitrotyrosine (N-Tyr) (all 1:1,000 dilution; Cell Signaling Technology, Allwil, Switzerland), SOD2 (1:2,000 dilution), Cat (1:10,000 dilution; both Abcam, Cambridge, UK), and TKT (1:200 dilution; Santa Cruz Biotechnologies) and incubation with peroxidase-conjugated secondary goat anti-rabbit, anti-mouse, or anti-goat antibody (1:3,000 dilution; Santa Cruz Biotechnologies). Protein bands were visualized using a commercial chemiluminescence detection kit (ECL Plus; Amersham Biosciences, Arlington Heights, IL) according to the manufacturer's protocol and exposure of the membrane to a film. Equal loading of the samples was demonstrated by reprobing membranes with β-actin antibody (Ms X Actin; Chemicon). The level of protein expression was quantified by the OptiQuant Acquisition Analysis Software (Microsoft XP).

Measurement of GSH content. About 0.5 cm colon tissue was homogenized in 125 mM Na_2HPO_4 and 6.3 mM EDTA, pH 7.5, and two repetitive freeze-thaw cycles in liquid nitrogen at 37°C. Lysate (40 μl) was transferred to a 96-well plate, and GSH standard samples of 0, 0.5, 1, 2, 5, 10, 15, 20, 250, and 500 μM were prepared for

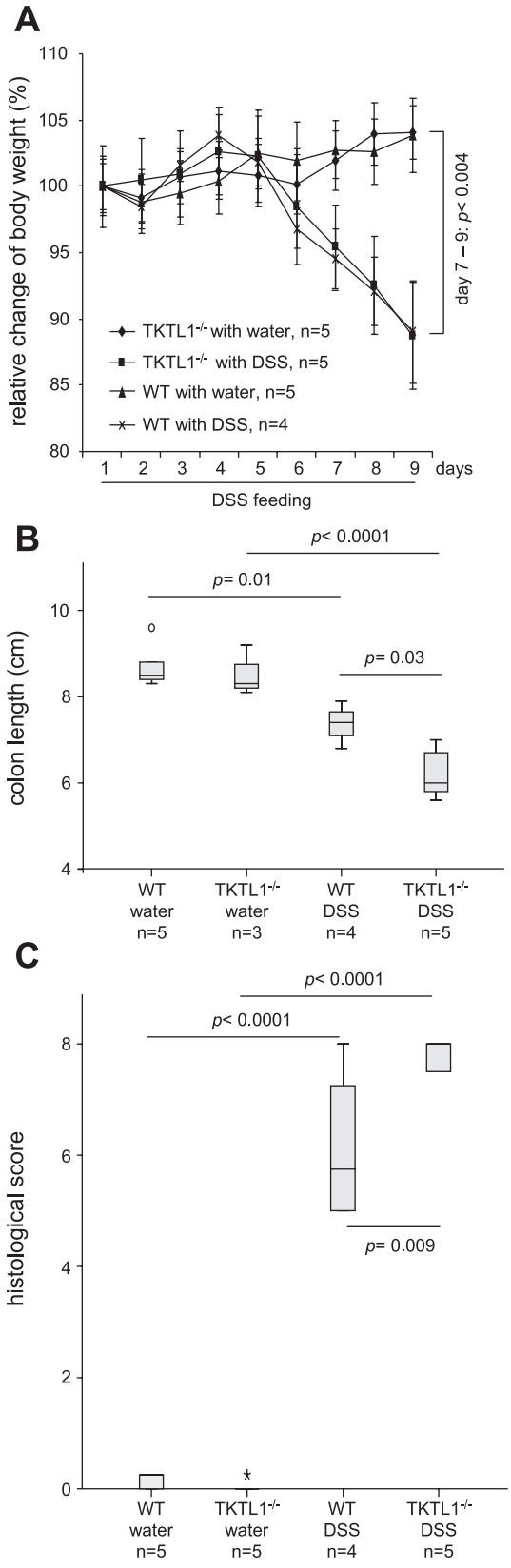

Fig. 4. Assessment of the clinical colitis parameter weight loss, colon shortening, and histological score during DSS-induced colitis. *A*: the weight loss was determined over 9 days. Weight progress is expressed as relative change of body weight in % to *day 1*. TKTL1$^{-/-}$ mice and WT mice with DSS-induced colitis lose significantly more weight compared with water control groups (*days 7–9*, $P < 0.004$, ANOVA). *B*: TKTL1$^{-/-}$ mice showed a significant reduction of colon length compared with WT mice during DSS treatment ($P = 0.03$, ANOVA).°Outlier. *C*: significantly higher total histological score indicating a more severe damage in TKTL1$^{-/-}$ mice compared with WT mice with DSS ($P = 0.009$, ANOVA). *Outlier.

standard curve determination. The reaction was initiated by addition of 170 μl of a reaction mix (14.56 ml distilled H_2O; 770 μl 0.5 M Tris·HCl, pH 7.5; 102.6 μl 150 mM glucose 6-phosphate, 9.24 μl 50 mM $NADP^+$, 2.5 ml 6 mM DTNB, 30 U glucose-6-phosphate dehydrogenase, and 30 U glutathione reductase). Absorbance was detected at 412 nm every 31 s for 5 min at 37°C by a Synergy 2 Multi Detection Microplate Reader (Witec, Littau, Switzerland).

Myeloperoxidase activity assay. Colon specimens were rinsed with 1× PBS and homogenized mechanically in 50 mM phosphate buffer (pH 6.0) and 0.5% hexadecyltrimethylammonium bromide (Sigma Aldrich) with a tissuelyzer (Qiagen). Three freeze and thaw cycles were performed. Homogenates were centrifuged for 2 min at maximum speed; 20 μl of the supernatant were transferred to a 96-well plate in duplicate and mixed with 280 μl of 0.02% dianisidine (in 50 mM phosphate buffer, pH 6.0, and 0.0005% H_2O_2; Sigma Aldrich). After 20 min, absorbance was measured at 460 nm. Protein concentration of the supernatant was determined by bicinchoninic acid protein assay. Myeloperoxidase (MPO) activity was calculated as mean absorbance (460 nm) per incubation time per protein concentration in grams (indicated as arbitrary units in Fig. 7*A*).

Data analysis and statistics. From each group, five animals could be analyzed (with the exception of the WT group, where analysis was performed on only 4 animals because of a low initial body weight of one animal at the beginning of the experiment). Statistical analysis of weight loss, colon length, histological score, and MPO was performed by ANOVA and a Post Hoc Multiple Comparison by Tukey. The MPO activity relative to water control as well as protein expression of TKT, iNOS, N-Tyr, SOD1, SOD2, and Cat data were analyzed by the Mann-Whitney test. IFN-γ, iNOS, TNF, IL-6, TKT mRNA, and GSH content were analyzed by the Kruskal Wallis test. Statistical significance was based on a P value <0.05.

RESULTS

Genotyping of TKTL1$^{-/-}$ mice and WT mice. Genomic DNA was extracted from total colon tissue for the discrimination between TKTL1$^{-/-}$ mice and WT mice.

TKTL1$^{-/-}$ mice showed a characteristic 338-bp fragment (Fig. 1*A*, *left*). WT mice showed no deletion of exon 4–7 and therefore no 338-bp fragment (Fig. 1*A*, *right*).

TKTL1$^{-/-}$ mice kept under normal conditions did not show any signs of intestinal pathology. They had a weight gain that was comparable to WT mice and had no clinical signs of mucosal inflammation (see Fig. 3, *A* and *E*, *I* and *II*). Histology of the intestinal mucosa was not different from WT mice (see Fig. 3, *B* and *F*, *I* and *II*). Therefore, we applied DSS to induce intestinal inflammation and investigate the role of TKTL1 during mucosal damage.

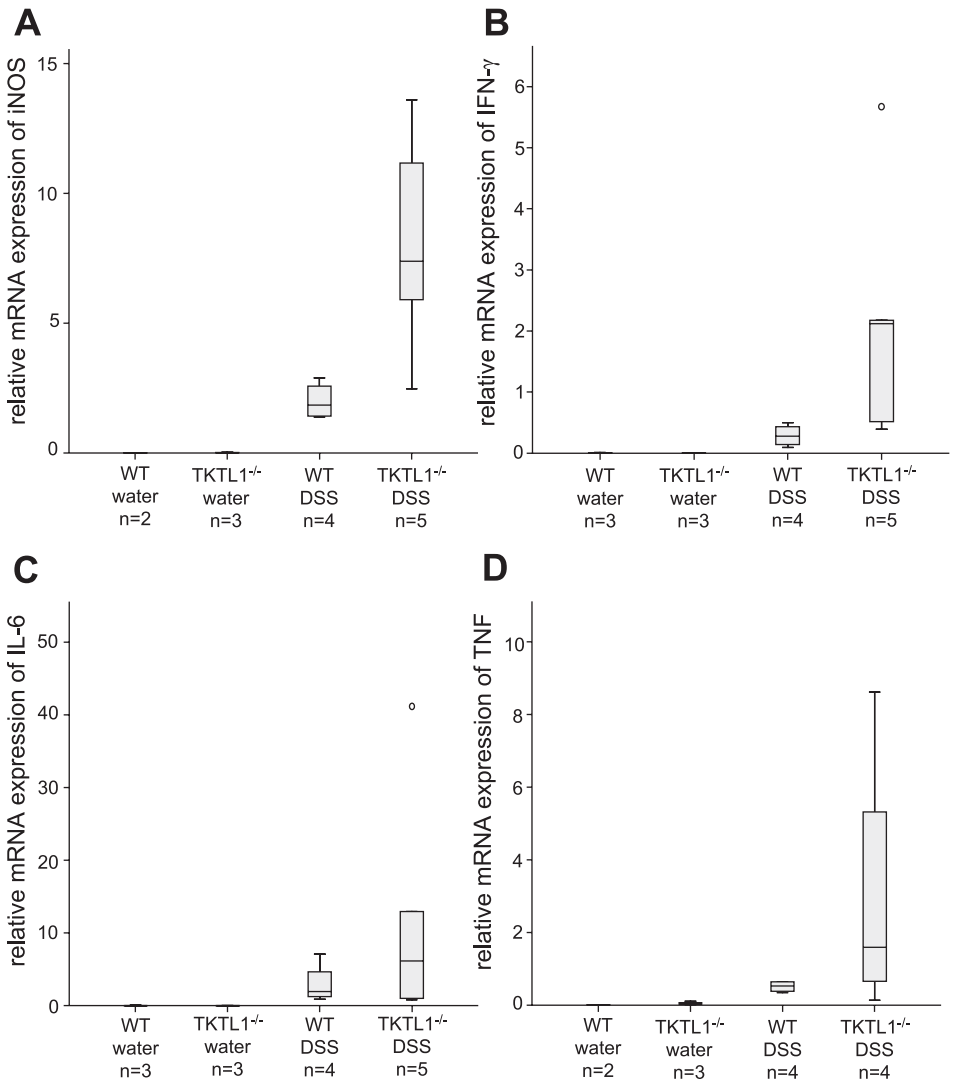

Fig. 5. mRNA expression of inducible nitric oxide synthase (iNOS, *A*), interferon (IFN)-γ (*B*), interleukin (IL)-6 (*C*), and tumor necrosis factor (TNF, *D*) in colon tissue samples of TKTL1$^{-/-}$ mice and WT mice with and without administration of DSS. Higher mRNA expression levels of iNOS, IFN-γ, IL-6, and TNF in the DSS group of TKTL1$^{-/-}$ mice compared with WT mice (not significant, Kruskal-Wallis test).°Outlier.

TKT mRNA and protein expression is not regulated in TKTL1$^{-/-}$ mice during DSS treatment. The constitutive knock out of TKTL1 could result in an upregulation of the TKT isoforms TKT and TKTL2. Determination of TKT and TKTL2 expression levels in colon specimens was carried out using semiquantitative PCR. Relative quantification to actin demonstrated that TKT is equally expressed in TKTL1$^{-/-}$ mice and WT mice whether DSS is administrated or not (TKTL1$^{-/-}$ vs. WT-DSS: no significant difference, Kruskal Wallis test; Fig. 1*B*).

TKTL2 is not expressed in colon tissue, either in TKTL1$^{-/-}$ mice or in WT mice (data not shown), which is in accordance with the literature (18).

TKT mRNA expression was also verified checking TKT protein expression by Western blotting (Fig. 2*A*). The normalization of TKT to β-actin protein expression demonstrated that there is no difference in TKT expression level in TKTL1$^{-/-}$ mice treated with DSS and WT mice treated with water or DSS. Moreover, TKTL1$^{-/-}$ mice showed no significantly different TKT protein expression compared with WT mice, both treated with DSS ($P = 0.773$, Mann-Whitney test; Fig. 2*B*). These findings indicate that TKT and TKTL2 are not upregulated to compensate for the lack of TKTL1.

TKTL1$^{-/-}$ mice have aggravated macroscopic mucosal damage upon DSS colitis. Mice received either DSS or water for 9 days. Macroscopic mucosal damage was assessed by miniendoscopy and evaluation by MEICS score (Fig. 3). The endoscopic colitis score MEICS indicated severe mucosal damage in TKTL1$^{-/-}$ mice with established DSS colitis (MEICS 11 ± 0, $n = 3$; Fig. 3*C*, *I* and *II*). Diseased regions often had a cobblestone-like appearance and mucosal bleeding. These findings were confirmed by histology (hematoxylin and eosin staining). Histology demonstrated a total loss of crypt structure in TKTL1$^{-/-}$ mice with DSS (Fig. 3*D*, *I* and *II*). In contrast, WT mice that received DSS (MEICS 10.5 ± 2.4, $n = 4$; Fig. 3G, *I* and *II*) demonstrated areas with degraded crypts and areas with an intact crypt pattern (Fig. 3*H*, *I* and *II*). Water control groups showed very weak signs of inflammation with a smooth and transparent mucosa and a normal vascular pattern (MEICS 0.1 ± 0.2, $n = 5$ and 0 ± 0, $n = 4$, respectively, Fig. 3*A*, *I* and *II*, and Fig. 3*E*, *I* and *II*). The mucosal surface appeared less granular compared with colitis mice, and the thickening of the colon was less prominent. Solid stool was visible. These findings were strengthened by the intact crypt structure in histology in both strains (Fig. 3*B*, *I* and *II*, and Fig. 3*F*, *I* and *II*). These macroscopic data show that TKTL1$^{-/-}$ mice with acute DSS-induced colitis had a negatively altered colonic mucosa.

Histology demonstrates worse inflammation in TKTL1$^{-/-}$ mice. The mice were examined for common parameters of colitis, including weight loss, shortening of the colon, and histological score. Both TKTL1$^{-/-}$ and WT mice that received DSS developed a severe inflammation measured by weight progression (Fig. 4*A*). From *day 7* until *day 9*, the weight of the groups treated with DSS was significantly lower than those of the corresponding water control groups ($P < 0.004$, ANOVA; Fig. 4*A*). However, there was no significant difference in weight between the two DSS-treated groups.

TKTL1$^{-/-}$ or WT mice, both treated with DSS, had a typical and significantly shorter colon than their corresponding water control groups (TKTL1$^{-/-}$: water vs. DSS, $P < 0.0001$; WT: water vs. DSS, $P = 0.01$, ANOVA; Fig. 4*B*). Moreover, TKTL1$^{-/-}$ mice had a significantly shorter colon than WT when both were treated with DSS ($P = 0.03$, ANOVA; Fig. 4*B*).

Microscopic mucosal damage and the inflammatory infiltrate were evaluated in a histological score (Fig. 4*C*). According to the assessed macroscopic mucosal damage, the total histolog-

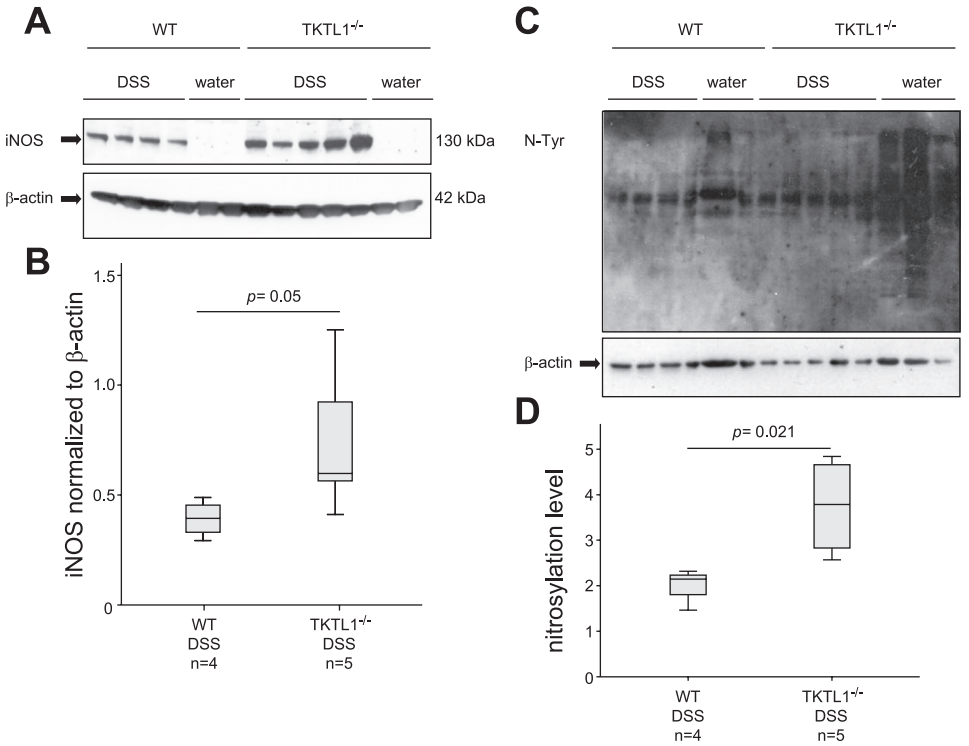

Fig. 6. *A*: Western blotting of iNOS in TKTL1$^{-/-}$ mice and WT mice. *B*: iNOS protein expression normalized to β-actin. TKTL1$^{-/-}$ mice expressed significantly more iNOS protein than WT mice ($P = 0.05$, Mann-Whitney test). *C*: Western blotting of nitrotyrosine (N-Tyr) in TKTL1$^{-/-}$ mice and WT mice. *D*: N-Tyr protein expression normalized to β-actin in TKTL1$^{-/-}$ mice and WT mice. There was enhanced nitrosylation in TKTL1$^{-/-}$ mice compared with WT mice during DSS treatment ($P = 0.021$, Mann-Whitney test).

ical score for TKTL1$^{-/-}$ mice (7.8 ± 0.1) with DSS was significantly increased compared with WT mice (6.1 ± 0.7) with DSS ($P = 0.009$, ANOVA). Water control mice showed almost no signs of inflammation; the total histological scores were 0.2 ± 0.06 and 0.05 ± 0.05 for TKTL1$^{-/-}$ mice and WT mice, respectively. TKTL1$^{-/-}$ mice had a significantly shorter colon and higher histological score than WT mice during DSS colitis.

iNOS, IFN-γ, IL-6, and TNF are increased in TKTL1$^{-/-}$ mice. We investigated the mRNA expression levels of the nitric oxide synthase iNOS and the proinflammatory cytokines IFN-γ, IL-6, and TNF in whole colon tissue of TKTL1$^{-/-}$ mice and WT mice with and without DSS to determine the severity of inflammation.

TKTL1$^{-/-}$ mice ($n = 3$) and WT mice ($n = 3$), which only received water, had low iNOS expression levels, 1.6 ± 0.8 and 0.7 ± 0.3, respectively (Fig. 5*A*), compared with DSS-treated animals. TKTL1$^{-/-}$ mice with DSS ($n = 5$) had a 4.1-fold induction of iNOS in contrast to WT mice with DSS ($n = 4$, not significant, Kruskal Wallis test).

TKTL1$^{-/-}$ mice ($n = 3$) and WT mice ($n = 3$) that only received water had very low IFN-γ expression levels, 0.2 ± 0.8 and 0.7 ± 0.2, respectively (Fig. 5*B*). TKTL1$^{-/-}$ mice with DSS ($n = 5$) had a 7.5-fold induction of IFN-γ in contrast to WT mice with DSS ($n = 4$, not significant, Kruskal Wallis test).

TKTL1$^{-/-}$ mice ($n = 3$) and WT mice ($n = 3$) that only received water had low IL-6 expression levels, 0.5 ± 0.2 and 1.6 ± 0.6, respectively (Fig. 5*C*), compared with DSS-treated animals. TKTL1$^{-/-}$ mice with DSS ($n = 5$) had a 4.2-fold induction of IL-6 in contrast to WT mice with DSS ($n = 4$, not significant, Kruskal Wallis test).

TKTL1$^{-/-}$ mice ($n = 3$) and WT mice ($n = 3$) that only received water had very low TNF expression levels, 5.4 ± 2.8 and 1.3 ± 0.3, respectively (Fig. 5*D*). TKTL1$^{-/-}$ mice with DSS ($n = 5$) had a 5.8-fold induction of TNF in contrast to WT mice with DSS ($n = 4$, not significant, Kruskal Wallis test). mRNA levels of iNOS, IFN-γ, IL-6, and TNF were increased in the DSS-fed groups compared with controls as well as in the TKTL1$^{-/-}$ DSS-treated mice compared with WT DSS-treated mice, but the increases were not significant.

iNOS protein expression and nitrosylation are enhanced in TKTL1$^{-/-}$ mice. The iNOS mRNA results were verified by Western blotting (Fig. 6*A*). Total protein was isolated from whole colon tissue of TKTL1$^{-/-}$ mice and WT mice treated with or without DSS.

TKTL1$^{-/-}$ mice ($n = 5$) showed a significantly higher iNOS protein expression than WT mice ($n = 4$) treated with DSS ($P = 0.05$, Mann-Whitney test; Fig. 6*B*). Water control groups ($n = 2$ each) of both strains showed no iNOS protein expression (Fig. 6*A*). The established mRNA data for iNOS were therefore verified by an enhanced iNOS protein expression in TKTL1$^{-/-}$ mice compared with WT mice fed with DSS.

The nitrosylation of tyrosine residues (N-Tyr) in proteins by NO potentially produced by iNOS was investigated by Western blotting (Fig. 6*C*). N-Tyr content was significantly enhanced in TKTL1$^{-/-}$ mice ($n = 5$) in contrast to WT mice ($n = 4$), both treated with DSS ($P = 0.021$, Mann-Whitney test; Fig. 6*D*). This indicates that reactive nitrogen species (RNS), which modify tyrosine residues in proteins, are elevated in TKTL1$^{-/-}$ mice compared with WT mice. However, the modification of proteins through the introduction of carbonyl groups by ROS is not enhanced in these animals (data not shown). Enhanced iNOS mRNA and protein expression correlates with an enhanced tyrosine residue modification in TKTL1$^{-/-}$ mice.

Activity of MPO is enhanced in TKTL1$^{-/-}$ mice in contrast to the antioxidative defense enzymes SOD1, SOD2, Cat, and GSH. To quantify the formation of ROS differentially, a MPO activity assay was used. MPO is a marker for tissue neutrophils in the assessment of inflammation.

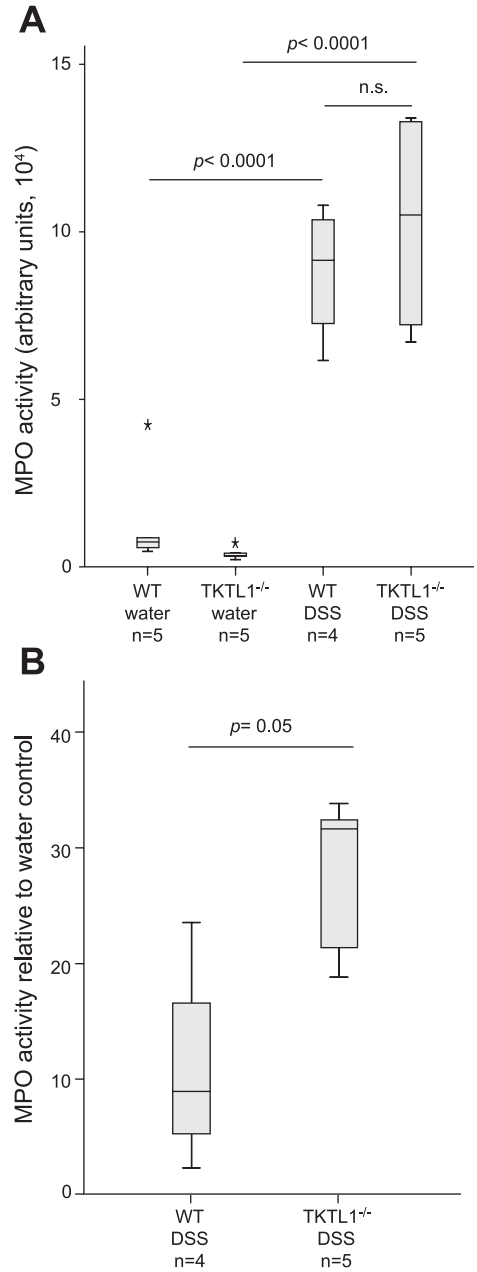

Fig. 7. *A*: myeloperoxidase (MPO) enzyme activity in mucosal homogenates of TKTL1$^{-/-}$ mice and WT mice with and without administration of DSS. There was a significantly higher MPO activity during DSS treatment in both groups compared with water control groups ($P < 0.0001$, ANOVA). ns, Not significant. *Outlier. *B*: the relative MPO activity of each DSS group to its corresponding water group resulted in a higher MPO activity in TKTL1$^{-/-}$ than WT mice ($P = 0.05$, Mann-Whitney test).

The homogenates of TKTL1$^{-/-}$ ($n = 5$) and WT ($n = 5$) water control mice showed a MPO activity of 3,961 ± 848 and 13,767 ± 7,181 arbitrary units (Fig. 7*A*, 2 left bars). In acute DSS-induced colitis (Fig. 7*A*, 2 left bars), MPO activity was significantly increased to 102,217 ± 14,277 arbitrary units in TKTL1$^{-/-}$ mice ($n = 5$) and 88,097 ± 10,156 arbitrary units in WT mice ($n = 4$) compared with water control groups. The MPO activity levels were significantly higher in DSS-fed groups compared with water control-fed groups (in both strains, $P < 0.0001$, ANOVA). The relative MPO activity of each DSS group to its corresponding water group resulted in a significantly higher MPO activity in TKTL1$^{-/-}$ mice in contrast to WT mice ($P = 0.05$, Mann-Whitney test; Fig. 7*B*). TKTL1$^{-/-}$ mice showed an increased susceptibility to experimental DSS colitis compared with WT, as confirmed by MPO activity. However, there is not a difference in the MPO activity comparing DSS-treated TKTL1$^{-/-}$ mice and DSS-treated WT mice.

Enzymatic antioxidants like superoxide dismutase (SOD), catalase (Cat), or glutathione (GSH) are crucial to maintain the redox balance in the cell and prevent damages by ROS. The production of H_2O_2 through the conversion of superoxides by SOD fuels the MPO reaction. Therefore, the expression of SOD1 and SOD2 was analyzed by Western blotting (Fig. 8, *A* and *C*). TKTL1$^{-/-}$ mice ($n = 5$) did not significantly express higher levels of SOD1 or SOD2 than WT mice ($n = 4$) fed with DSS ($P = 0.480$ and $P = 0.773$, Mann-Whitney test; Fig. 8, *B* and *D*). Produced H_2O_2 may also further be scavenged by Cat, which subsequently converts it to O_2 and H_2O. Protein expression of Cat was therefore also analyzed by Western blotting (Fig. 8*E*). TKTL1$^{-/-}$ mice demonstrated no significantly higher Cat expression than WT mice treated with DSS ($P = 0.773$, Mann-Whitney test; Fig. 8*F*). GSH as one of the major regulating systems of the redox status of the cell was measured in colon specimens (Fig. 8*G*). GSH content was not significantly reduced in TKTL1$^{-/-}$ mice compared with WT mice treated with water or DSS (Kruskal Wallis test). The antioxidative defense enzymes SOD1, SOD2, Cat, and GSH are not significantly changed in TKTL1$^{-/-}$ mice compared with WT mice under inflammatory conditions.

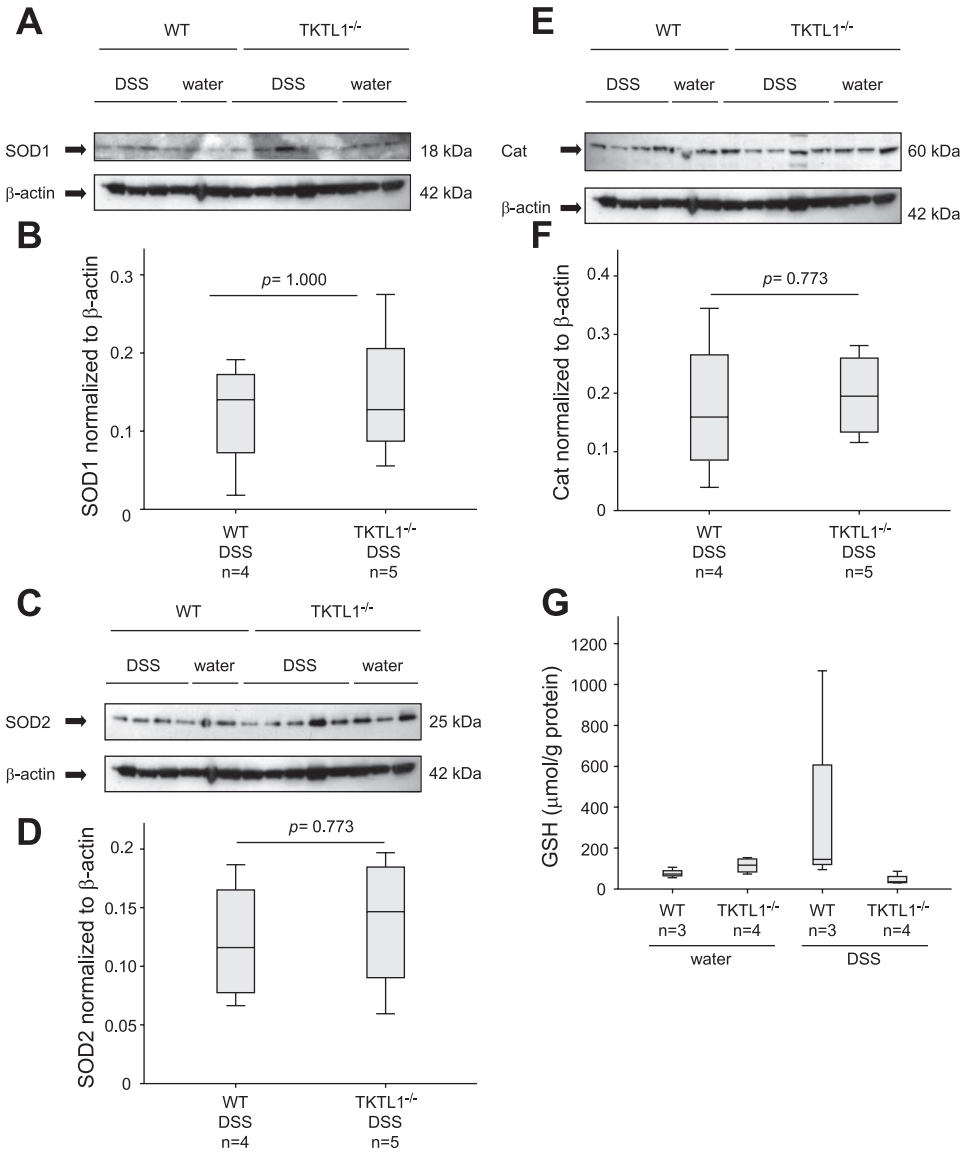

Fig. 8. *A*: superoxide dismutase 1 (SOD1) protein expression in TKTL1$^{-/-}$ mice and WT mice with and without administration of DSS. *B*: SOD1 protein expression normalized to β-actin. There was no significantly higher SOD1 expression during DSS treatment in TKTL1$^{-/-}$ mice compared with WT mice ($P = 1.000$, Mann-Whitney test). *C*: superoxide dismutase 2 (SOD2) protein expression in TKTL1$^{-/-}$ mice and WT mice with and without administration of DSS. *D*: SOD2 protein expression normalized to β-actin. There was no significantly higher SOD2 expression during DSS treatment in TKTL1$^{-/-}$ mice compared with WT mice ($P = 0.773$, Mann-Whitney test). *E*: catalase (Cat) protein expression in TKTL1$^{-/-}$ mice and WT mice with and without administration of DSS. *F*: Cat protein expression normalized to β-actin. There was no significantly higher Cat expression during DSS treatment in TKTL1$^{-/-}$ mice compared with WT mice ($P = 0.773$, Mann-Whitney test). *G*: glutathione (GSH) content in colon tissue of TKTL1$^{-/-}$ mice compared with WT mice. There was no difference between TKTL1$^{-/-}$ mice and WT mice whether during water or DSS treatment (not significant, Kruskal-Wallis test).

DISCUSSION

The constitutive knock out of TKTL1 did not influence the expression of transketolase isoforms TKT and TKTL2 whether DSS was given or not. The induction of DSS colitis in TKTL1$^{-/-}$ mice and WT mice resulted in significant weight loss and colon shortening compared with water control mice in both strains as well as severe mucosal damage estimated by histology in TKTL1$^{-/-}$ mice compared with WT mice. The susceptibility to DSS, measured by the expression of iNOS, was significantly increased in TKTL1$^{-/-}$ mice. The activity of the MPO enzyme was elevated under the inflammatory conditions in TKTL1$^{-/-}$ mice in contrast to WT mice. The antioxidative enzymes SOD1, SOD2, Cat, GSH as well as carbonylation of proteins were not elevated in TKTL1$^{-/-}$ mice. However, the modification of tyrosine residues due to higher RNS challenging was enhanced in TKTL1$^{-/-}$ mice in contrast to WT mice, reflecting higher oxidative stress conditions in these mice. Our work is the first that examines the effect of an inactivation of TKTL1 during inflammation.

A predisposition to oxidative damage after the loss of total TKTs activity was seen in corneal cells of the mouse (34), rabbit, and humans (19). The depletion of NADPH may contribute to the damage of corneal cells (19). In bovine corneal epithelium, 35% of glucose is metabolized via the PPP (16). Normally, expression of TKT increases in corneas during the time of eyelid opening (34) and is upregulated by exposure to light and oxidative stress conditions (35). Presumably, this high activity reflects the need of the corneal tissue for sufficient amounts of reducing equivalents like NADPH for the prevention of damage by free radicals formed by ultraviolet radiation (8, 34). In addition, enzymatic activity of TKT in the PPP also provides the NADPH cofactor for other ARE-linked gene products (27), such as glutathione reductase, aldo-keto reductase, quinone reductase, and thioredoxin reductase, which ameliorates oxidative stress as well (20). The authors could not exclude that there may be a synergistic effect of TKT and these ARE-linked genes.

Although the production of NADPH takes place in the oxidative part of the PPP, a further downstream blockage of TKTL1 could influence the biochemical balance leading to reduced NADPH production and an impaired defense against oxidative stress. This has already been demonstrated in colon epithelial cells (HCT116) in vitro (44). Their finding of a reduction of intracellular NADPH and GSH concentrations and a subsequently much weaker ROS defense was shown by short-hairpin (sh) RNA-mediated knock down of TKTL1. Xu and colleagues (44) assumed that TKTL1 seemed to have a protective effect against oxidative or radical stress. The disturbance of the biochemical balance resulting from the shRNA-mediated blockage of TKTL1 seems to affect the NADPH production in the oxidative part of the PPP and reverses the protective effect against oxidative or radical stress. Moreover, Xue et al. (46) investigated the deprivation of TKT through small-interfering RNA knockdown in endothelial cells (HMEC-1), which also resulted in a direct increase in ROS formation. This study concluded that a knock out in vivo also could result in increased ROS formation.

The protective role of the PPP against oxidative stress has been also investigated in yeast, *S. cerevisiae*, which contains the same oxidative stress defense mechanisms present in higher eukaryotes (23). This model has shown TKT to be a critical enzyme involved in the cellular defense against oxidative damage (39). Moreover, *S. cerevisiae* strains deleted for TKTL1 are sensitive to H_2O_2 (15, 43) and also defective in adaptation to H_2O_2 (26).

A depletion of reducing agents in the etiology of inflammatory conditions, such as IBD, has previously been proposed. Levels of the most important antioxidants have been found to be seriously impaired within the intestinal mucosa from IBD patients compared with normal mucosa (17). Furthermore, increased ROS levels are thought to play an important role in maintaining or promoting the phenotype of cancer cells (10). An established fact is that patients with long-standing ulcerative colitis are at an increased risk of developing colorectal cancer (40). A lack of TKTL1 in these patients may therefore promote the transformation of the cells in a cancer cell phenotype. Several antioxidative drugs have been successfully used for the treatment of ulcerative colitis (13, 29) or DSS-induced colitis (9). Obermeier and colleagues (28) demonstrated that IFN-γ and TNF have a damaging effect via the induction of iNOS and the toxic effector molecule NO. An excessive $NO^{\bullet}$ production by iNOS has been implicated in decreased mucosal barrier function (3). Inhibition of iNOS has consistently shown positive effects in animal models of intestinal inflammation (25, 31). Therefore, the higher iNOS expression in this study could lead to a higher damage in barrier function in TKTL1$^{-/-}$ mice.

In conclusion, our results demonstrate that an inactivation of TKTL1 in mice leads to increased inflammation in experimental DSS colitis.

ACKNOWLEDGMENTS

We thank Dr. Jyrki Eloranta (Division of Clinical Pharmacology and Toxicology, University Hospital Zurich, Zurich, Switzerland) for critically reading the manuscript.

Parts of this study were orally presented at the Digestive Disease Week in New Orleans, LA, in 2010.

GRANTS

This study was supported by Grants SNF 310030-120312 to G. Rogler and BioChancePlus/0315364 by the Bundesministerium für Forschung und Bildung. S. Bentz is a member of the PhD program of the Zurich Center for Integrative Human Physiology in Zurich, Switzerland.

DISCLOSURES

The author J. F. Coy declares a potential conflict of interest due to the possible utilization of TKTL1 for diagnostic and/or therapeutic purposes.

REFERENCES

1. **Becker C, Fantini MC, Neurath MF.** High resolution colonoscopy in live mice. *Nat Protoc* 1: 2900–2904, 2006.
2. **Boughton-Smith NK, Evans SM, Hawkey CJ, Cole AT, Balsitis M, Whittle BJ, Moncada S.** Nitric oxide synthase activity in ulcerative colitis and Crohn's disease. *Lancet* 342: 338–340, 1993.
3. **Chavez AM, Menconi MJ, Hodin RA, Fink MP.** Cytokine-induced intestinal epithelial hyperpermeability: role of nitric oxide. *Crit Care Med* 27: 2246–2251, 1999.
4. **Coy JF, Dressler D, Wilde J, Schubert P.** Mutations in the transketolase-like gene TKTL1: clinical implications for neurodegenerative diseases, diabetes and cancer. *Clin Lab* 51: 257–273, 2005.
5. **Coy JF, Dubel S, Kioschis P, Thomas K, Micklem G, Delius H, Poustka A.** Molecular cloning of tissue-specific transcripts of a transketolase-related gene: implications for the evolution of new vertebrate genes. *Genomics* 32: 309–316, 1996.

6. **Furuta E, Okuda H, Kobayashi A, Watabe K.** Metabolic genes in cancer: their roles in tumor progression and clinical implications. *Biochim Biophys Acta* 1805: 141–152, 2010.
7. **Grisham MB, Yamada T.** Neutrophils, nitrogen oxides, and inflammatory bowel disease. *Ann NY Acad Sci* 664: 103–115, 1992.
8. **Guo J, Sax CM, Piatigorsky J, Xu FX.** Heterogeneous expression of transketolase in ocular tissues. *Curr Eye Res* 16: 467–474, 1997.
9. **Hausmann M, Obermeier F, Paper DH, Balan K, Dunger N, Menzel K, Falk W, Schoelmerich J, Herfarth H, Rogler G.** In vivo treatment with the herbal phenylethanoid acteoside ameliorates intestinal inflammation in dextran sulphate sodium-induced colitis. *Clin Exp Immunol* 148: 373–381, 2007.
10. **Hu Y, Rosen DG, Zhou Y, Feng L, Yang G, Liu J, Huang P.** Mitochondrial manganese-superoxide dismutase expression in ovarian cancer: role in cell proliferation and response to oxidative stress. *J Biol Chem* 280: 39485–39492, 2005.
11. **Huang EH, Carter JJ, Whelan RL, Liu YH, Rosenberg JO, Rotterdam H, Schmidt AM, Stern DM, Forde KA.** Colonoscopy in mice. *Surg Endosc* 16: 22–24, 2002.
12. **Ishihara T, Tanaka K, Tasaka Y, Namba T, Suzuki J, Ishihara T, Okamoto S, Hibi T, Takenaga M, Igarashi R, Sato K, Mizushima Y, Mizushima T.** Therapeutic effect of lecithinized superoxide dismutase against colitis. *J Pharmacol Exp Ther* 328: 152–164, 2009.
13. **Isozaki Y, Yoshida N, Kuroda M, Takagi T, Handa O, Kokura S, Ichikawa H, Naito Y, Okanoue T, Yoshikawa T.** Effect of a novel water-soluble vitamin E derivative as a cure for TNBS-induced colitis in rats. *Int J Mol Med* 17: 497–502, 2006.
14. **Jeyasingham MD, Pratt OE, Shaw GK, Thomson AD.** Changes in the activation of red blood cell transketolase of alcoholic patients during treatment. *Alcohol Alcohol* 22: 359–365, 1987.
15. **Juhnke H, Krems B, Kotter P, Entian KD.** Mutants that show increased sensitivity to hydrogen peroxide reveal an important role for the pentose phosphate pathway in protection of yeast against oxidative stress. *Mol Gen Genet* 252: 456–464, 1996.
16. **Kinoshita JH, Masurat T, Helfant M.** Pathways of glucose metabolism in corneal epithelium. *Science* 122: 72–73, 1955.
17. **Kruidenier L, Kuiper I, Lamers CB, Verspaget HW.** Intestinal oxidative damage in inflammatory bowel disease: semi-quantification, localization, and association with mucosal antioxidants. *J Pathol* 201: 28–36, 2003.
18. **Langbein S, Zerilli M, Zur Hausen A, Staiger W, Rensch-Boschert K, Lukan N, Popa J, Ternullo MP, Steidler A, Weiss C, Grobholz R, Willeke F, Alken P, Stassi G, Schubert P, Coy JF.** Expression of transketolase TKTL1 predicts colon and urothelial cancer patient survival: Warburg effect reinterpreted. *Br J Cancer* 94: 578–585, 2006.
19. **Lassen N, Black WJ, Estey T, Vasiliou V.** The role of corneal crystallins in the cellular defense mechanisms against oxidative stress. *Semin Cell Dev Biol* 19: 100–112, 2008.
20. **Lee JM, Calkins MJ, Chan K, Kan YW, Johnson JA.** Identification of the NF-E2-related factor-2-dependent genes conferring protection against oxidative stress in primary cortical astrocytes using oligonucleotide microarray analysis. *J Biol Chem* 278: 12029–12038, 2003.
21. **MacDonald TT, Hutchings P, Choy MY, Murch S, Cooke A.** Tumour necrosis factor-alpha and interferon-gamma production measured at the single cell level in normal and inflamed human intestine. *Clin Exp Immunol* 81: 301–305, 1990.
22. **Miller MJ, Thompson JH, Zhang XJ, Sadowska-Krowicka H, Kakkis JL, Munshi UK, Sandoval M, Rossi JL, Eloby-Childress S, Beckman JS.** Role of inducible nitric oxide synthase expression and peroxynitrite formation in guinea pig ileitis. *Gastroenterology* 109: 1475–1483, 1995.
23. **Moradas-Ferreira P, Costa V, Piper P, Mager W.** The molecular defences against reactive oxygen species in yeast. *Mol Microbiol* 19: 651–658, 1996.
24. **Murata Y, Ishiguro Y, Itoh J, Munakata A, Yoshida Y.** The role of proinflammatory and immunoregulatory cytokines in the pathogenesis of ulcerative colitis. *J Gastroenterol Suppl* 8: 56–60, 1995.
25. **Neilly PJ, Gardiner KR, Rowlands BJ.** Experimental colitis is ameliorated by inhibition of nitric oxide synthase activity (Abstract). *Gut* 38: 475, 1996.
26. **Ng CH, Tan SX, Perrone GG, Thorpe GW, Higgins VJ, Dawes IW.** Adaptation to hydrogen peroxide in Saccharomyces cerevisiae: the role of NADPH-generating systems and the SKN7 transcription factor. *Free Radic Biol Med* 44: 1131–1145, 2008.
27. **Nixon PF, Kaczmarek MJ, Tate J, Kerr RA, Price J.** An erythrocyte transketolase isoenzyme pattern associated with the Wernicke-Korsakoff syndrome. *Eur J Clin Invest* 14: 278–281, 1984.
28. **Obermeier F, Kojouharoff G, Hans W, Scholmerich J, Gross V, Falk W.** Interferon-gamma (IFN-gamma)- and tumour necrosis factor (TNF)-induced nitric oxide as toxic effector molecule in chronic dextran sulphate sodium (DSS)-induced colitis in mice. *Clin Exp Immunol* 116: 238–245, 1999.
29. **Oz HS, Chen TS, McClain CJ, de Villiers WJ.** Antioxidants as novel therapy in a murine model of colitis. *J Nutr Biochem* 16: 297–304, 2005.
30. **Pannunzio P, Hazell AS, Pannunzio M, Rao KV, Butterworth RF.** Thiamine deficiency results in metabolic acidosis and energy failure in cerebellar granule cells: an in vitro model for the study of cell death mechanisms in Wernicke's encephalopathy. *J Neurosci Res* 62: 286–292, 2000.
31. **Rachmilewitz D, Karmeli F, Okon E, Bursztyn M.** Experimental colitis is ameliorated by inhibition of nitric oxide synthase activity. *Gut* 37: 247–255, 1995.
32. **Reinecker HC, Steffen M, Witthoeft T, Pflueger I, Schreiber S, MacDermott RP, Raedler A.** Enhanced secretion of tumour necrosis factor-alpha, IL-6, and IL-1 beta by isolated lamina propria mononuclear cells from patients with ulcerative colitis and Crohn's disease. *Clin Exp Immunol* 94: 174–181, 1993.
33. **Ribbons KA, Zhang XJ, Thompson JH, Greenberg SS, Moore WM, Kornmeier CM, Currie MG, Lerche N, Blanchard J, Clark DA.** Potential role of nitric oxide in a model of chronic colitis in rhesus macaques. *Gastroenterology* 108: 705–711, 1995.
34. **Sax CM, Salamon C, Kays WT, Guo J, Yu FX, Cuthbertson RA, Piatigorsky J.** Transketolase is a major protein in the mouse cornea. *J Biol Chem* 271: 33568–33574, 1996.
35. **Sax CM, Kays WT, Salamon C, Chervenak MM, Xu YS, Piatigorsky J.** Transketolase gene expression in the cornea is influenced by environmental factors and developmentally controlled events. *Cornea* 19: 833–841, 2000.
36. **Schenk G, Duggleby RG, Nixon PF.** Properties and functions of the thiamin diphosphate dependent enzyme transketolase. *Int J Biochem Cell Biol* 30: 1297–1318, 1998.
37. **Schmid U, Stopper H, Heidland A, Schupp N.** Benfotiamine exhibits direct antioxidative capacity and prevents induction of DNA damage in vitro. *Diabetes Metab Res Rev* 24: 371–377, 2008.
38. **Shangari N, Mehta R, O'Brien PJ.** Hepatocyte susceptibility to glyoxal is dependent on cell thiamin content. *Chem Biol Interact* 165: 146–154, 2007.
39. **Slekar KH, Kosman DJ, Culotta VC.** The yeast copper/zinc superoxide dismutase and the pentose phosphate pathway play overlapping roles in oxidative stress protection. *J Biol Chem* 271: 28831–28836, 1996.
40. **Stallmach A, Bielecki C, Schmidt C.** Malignant transformation in inflammatory bowel disease–surveillance guide. *Dig Dis* 27: 584–590, 2009.
41. **Steidler L, Hans W, Schotte L, Neirynck S, Obermeier F, Falk W, Fiers W, Remaut E.** Treatment of murine colitis by Lactococcus lactis secreting interleukin-10. *Science* 289: 1352–1355, 2000.
42. **Sun W, Liu Y, Glazer CA, Shao C, Bhan S, Demokan S, Zhao M, Rudek MA, Ha PK, Califano JA.** TKTL1 is activated by promoter hypomethylation and contributes to head and neck squamous cell carcinoma carcinogenesis through increased aerobic glycolysis and HIF1alpha stabilization. *Clin Cancer Res* 16: 857–866, 2010.
43. **Thorpe GW, Fong CS, Alic N, Higgins VJ, Dawes IW.** Cells have distinct mechanisms to maintain protection against different reactive oxygen species: oxidative-stress-response genes. *Proc Natl Acad Sci USA* 101: 6564–6569, 2004.
44. **Xu X, Zur Hausen A, Coy JF, Lochelt M.** Transketolase-like protein 1 (TKTL1) is required for rapid cell growth and full viability of human tumor cells. *Int J Cancer* 124: 1330–1337, 2009.
45. **Xu ZP, Wawrousek EF, Piatigorsky J.** Transketolase haploinsufficiency reduces adipose tissue and female fertility in mice. *Mol Cell Biol* 22: 6142–6147, 2002.
46. **Xue M, Qian Q, Adaikalakoteswari A, Rabbani N, Babaei-Jadidi R, Thornalley PJ.** Activation of NF-E2-related factor-2 reverses biochemical dysfunction of endothelial cells induced by hyperglycemia linked to vascular disease. *Diabetes* 57: 2809–2817, 2008.